Is the H_2OCl^+ Ion a Viable Intermediate for the Hydrolysis of $ClONO_2$ on Ice Surfaces?

Roberto Bianco,[†] Ward H. Thompson,[†,‡] Akihiro Morita,[†,§] and James T. Hynes*[,†,||]

Department of Chemistry and Biochemistry, University of Colorado, Boulder, Colorado 80309-0215, and Département de Chimie, CNRS UMR 8640, Ecole Normale Supérieure, 24 rue Lhomond, Paris 75231, France

Received: July 21, 2000; In Final Form: January 25, 2001

The involvement of the H_2OCl^+ ion in the $ClONO_2$ hydrolysis on an ice surface is shown to be unlikely via quantum chemical calculations and comparative analysis of infrared spectra of low temperature mixtures of H_2O with HNO_3, N_2O_5 or $ClONO_2$. For the $ClONO_2$ hydrolysis on ice, the reaction path involving H_2OCl^+ is estimated to be ∼10−14 kcal/mol higher in energy than the one involving H_3O^+ via proton transfer in the ice lattice. An analysis of literature infrared spectra, complemented by quantum chemical calculations of the vibrational frequencies of the relevant species, indicates that the spectral feature previously assigned to H_2OCl^+ should instead be assigned to molecular HNO_3.

1. Introduction

The study of chemical reactions at ice surfaces important in ozone depletion is evolving from initial experimental studies aimed at assessing their viability toward an understanding of the fundamental reaction pathways involved. Stemming from the demonstrated ability of an ice surface to promote reactions otherwise unlikely in the gas phase, attention has recently focused on the role of the ice lattice. In particular, the $ClONO_2$ hydrolysis on ice

$$ClONO_2 + H_2O \xrightarrow{\text{ice}} HOCl + HNO_3 \qquad (1.1)$$

has been investigated both experimentally[1−18] and theoretically[19−26] to uncover the mechanism and assess the role of the ice lattice. This reaction is important as a possible first step in the reaction of HCl with $ClONO_2$[1−16] and also of independent interest as a source of HOCl.[2,9,10,13] Two molecular level mechanisms, markedly different in character, have been proposed for reaction (1.1).[11,20] Here, we present several considerations to assist in the resolution of this issue.

It is known that the reaction involves a nucleophilic attack of a water oxygen on the chlorine in $ClONO_2$, breaking the $Cl-ONO_2$ bond.[7] Sodeau et al[11] (SHBK) have proposed, based on the analysis of reflection−absorption infrared (RAIR) spectra, that (1.1) occurs via the two step mechanism

$$H_2O + ClONO_2 \rightarrow H_2OCl^+NO_3^- \qquad (1.2)$$

$$H_2OCl^+NO_3^- + H_2O \rightarrow H_3O^+ + HOCl + NO_3^- \qquad (1.3)$$

involving the nucleophilic attack of a neutral water molecule on Cl in $ClONO_2$ which would generate the H_2OCl^+ reactive intermediate.[12,27]

Bianco and Hynes[20] (BH) pointed out, however, that a water molecule is not likely to be a nucleophile strong enough to carry out a facile attack on $ClONO_2$,[28] an argument against the feasibility of (1.2), even taking into account solvation effects. In this connection, the existence of the species $[H_2OX]^+$ (X = Cl and Br) was ruled out in experimental aqueous solution studies of the halogen hydrolysis reactions $X_2 + H_2O \rightarrow XOH + H^+ + X^-$.[29] BH, via quantum chemical reaction path calculations on the mechanism of reaction (1.1) on ice, found instead that the attacking water becomes an OH^--like moiety—a nucleophile much stronger than H_2O[28]—by transferring a proton to the ice lattice. A schematic representation of this view is the single step mechanism

$$H_2O{\cdot}H_2O{\cdot}ClONO_2(ads) \rightarrow [H_2O\cdots H^{\delta+}\cdots HO^{\delta-}\cdots Cl^{\delta+}\cdots ONO_2{}^{\delta-}]^{\dagger}(ads) \rightarrow H_2OH^+{\cdot}HOCl{\cdot}ONO_2{}^-(ads) \qquad (1.4)$$

where the proton transfer and the nucleophilic attack are coupled. A further non-rate-limiting proton transfer in a water chain (not shown) was found by BH to produce a $H_3O^+{\cdot}NO_3^-$ contact ion pair, displayed later within. In addition, solvating waters (not displayed) play an important role in stabilizing the transition state;[20] the calculated barrier of about 3 kcal/mol[20] for the ionic mechanism described is close to experimental estimates.[30,31]

In the BH study, it was also found that, although the calculations indicated significant interaction between the model ice lattice and $ClONO_2$, with a marked polarization of the reactant $ClONO_2$ molecule, the $H_2OCl^+NO_3^-$ ion pair proposed by SHBK was not identifiable along the calculated reaction path. Further, the quantum chemical calculation of a hypothetical reaction path where the proton transfer from the attacking water was forbidden,[21] like in the first step of the SHBK mechanism, eq 1.2, yielded a pathway far higher in energy than that from a comparable calculation where instead proton transfer was naturally allowed.

As is further discussed within, the original SHBK proposal hinges upon a certain analysis of the spectra of a $ClONO_2/H_2O$ 10:1 mixture and a N_2O_5/H_2O 1:10 mixture at 180 K in the

* To whom correspondence should be addressed. E-mail: hynes@spot.colorado.edu. Fax: +303 492 5894.
† University of Colorado.
‡ Current address: Department of Chemistry, University of Kansas, Lawrence, KS 66045.
§ Current address: Department of Chemistry, Kyoto University, Kyoto 606-8502, Japan.
|| Ecole Normale Supérieure.

10.1021/jp002599v CCC: $20.00
Published on Web 03/02/2001

1600−1800 cm^{-1} region, which would indicate, according to SHBK, the presence of the H_2OCl^+ ion in the $ClONO_2/H_2O$ mixture. By an examination of these same spectra, BH have argued against this and offered some evidence for the presence of molecular HNO_3 in lieu of H_2OCl^+. In addition, experimental observations by Oppliger et al.[8] on the mechanism of the $ClONO_2$ hydrolysis on ice, initially interpreted by invoking a $H_2OCl^+ \cdot NO_3^-$ contact ion pair, have been successfully explained via the BH mechanism.[17,20] In subsequent work, Sodeau and co-workers[13,14] have suggested that the BH mechanism is possibly only applicable at low temperatures (less than 145 K), where the existence of H_2OCl^+ is no longer claimed,[13,14]but still maintain the SHBK mechanism near stratospherically relevant temperatures (∼190 K).

For some time now, the invocation of the H_2OCl^+ ion has continued in the literature. Its existence on ice surfaces is often taken for granted and used in the interpretation of recent work on $ClONO_2$ hydrolysis on ice and related systems by some authors,[8,13,18,25−27] while tentatively accepted by others.[24] In our view, the early inference of the involvement of H_2OCl^+ [11] lacks both experimental and theoretical support. Thus, we have considered it valuable to address the issue from both new theoretical and spectroscopic viewpoints. In section 2, we discuss thermodynamic cycles aimed at evaluating the feasibility of a $ClONO_2$ hydrolysis mechanism involving the H_2OCl^+ ion. In section 3, in an analysis of various experimental spectra, we compare the infrared signature previously assigned to H_2OCl^+ with those of HNO_3, H_3O^+, and NO_3^- on ice surfaces. In section 4, we calculate the infrared absorption patterns of HNO_3 and the $H_3O^+ \cdot NO_3^-$ contact ion pair in water clusters and compare them to the experimental spectra. Concluding remarks, focused on suggested experiments, are offered in section 5.

2. Thermodynamic Cycles for the $ClONO_2$ Hydrolysis on Ice

We can estimate the enthalpy of reaction for the two different mechanisms for $ClONO_2$ hydrolysis discussed in the Introduction using a combination of thermochemical data available in the literature and ab initio calculations. In mechanism I, proposed by BH, the reaction proceeds via the nucleophilic attack of a water molecule concerted with the proton transfer from this water to the ice lattice, leading to a $H_3O^+ \cdot NO_3^-$ contact ion pair

$$ClONO_2(aq) + 3H_2O(aq) \rightarrow HOCl \cdot NO_3^- \cdot H_3O^+ \cdot H_2O(aq) \quad (2.5)$$

Consistent with BH's proposed mechanism, we include three water molecules in the equations. Mechanism II, proposed by SHBK, involves the same nucleophilic attack but without any assisting proton transfer and leads to a $H_2OCl^+ \cdot NO_3^-$ contact ion pair

$$ClONO_2(aq) + 3H_2O(aq) \rightarrow H_2OCl^+ \cdot NO_3^- \cdot H_2O \cdot H_2O(aq) \quad (2.6)$$

Note that the final products we are considering here are product complexes in condensed phase.

As a starting point, we first consider the analogous reactions occurring in the gas phase, which allows us to use the established thermochemical data for the species involved. We first consider mechanism I, which in the gas-phase proceeds as

TABLE 1: Thermodynamic Data for the $ClONO_2$ Hydrolysis[a]

species	$\Delta H_{f,298}$[b]	IP[b]	EA[b]	PA
Cl^+	328		12.967	
H^+	365.7			
HOCl	−19	11.12		153.1[c]
H_2OCl^+	193.6[d]			
H_2O	−57.8	12.612		166.9
H_3O^+	141			
NO_3^-	−73.4			
HNO_3	−32	11.95		
$ClONO_2$	5.5			

[a] $\Delta H_{f,298}$: enthalpy of formation at 298 K in kcal/mol. IP: ionization potential in eV. EA: electron affinity in eV. PA: proton affinity in kcal/mol. [b] Reference 32, unless otherwise indicated. [c] Reference 33. [d] Obtained as $\Delta H_f(H_2OCl^+) = -\mathrm{PA}(HOCl) + \Delta H_f(H^+) + \Delta H_f(HOCl)$.

$$ClONO_2(g) + 3H_2O(g) \rightarrow HOCl(g) + NO_3^-(g) + H_3O^+(g) + H_2O(g) \quad (2.7)$$

The enthalpy of this reaction is estimated, using the data in Table 1, to be $\Delta H_I^g = 158.7$ kcal/mol, where the superscript g indicates the gas-phase reaction. The reaction enthalpy for mechanism II can be evaluated in the same way. The gas-phase reaction is

$$ClONO_2(g) + 3H_2O(g) \rightarrow H_2OCl^+(g) + NO_3^-(g) + 2H_2O(g) \quad (2.8)$$

with a reaction enthalpy $\Delta H_{II}^g = 172.5$ kcal/mol. The enthalpy difference of 13.8 kcal/mol for the two gas-phase reactions favors mechanism I and reflects the higher gas-phase proton affinity of H_2O compared to HOCl (see Table 1). The question is now: can this intrinsic bias favoring mechanism I over mechanism II be overcome by complexation and solvation effects for the reactions?

The enthalpy differences associated with the effects of clustering and solvating the products for the two mechanisms can be evaluated via ab initio calculations and included in the corresponding reaction cycles. Thus, e.g., for mechanism I

$$ClONO_2(aq) + 3H_2O(aq) \xrightarrow{-\Delta H_I^{sr}} ClONO_2(g) + 3H_2O(g)$$

$$ClONO_2(g) + 3H_2O(g) \xrightarrow{\Delta H_I^g} HOCl(g) + NO_3^-(g) + H_3O(g)^+ + H_2O(g)$$

$$HOCl(g) + NO_3^-(g) + H_3O^+(g) + H_2O(g) \xrightarrow{\Delta H_I^{sp}} HOCl \cdot NO_3^- \cdot H_3O^+ \cdot H_2O(aq) \quad (2.9)$$

$$ClONO_2(aq) + 3H_2O(aq) \xrightarrow{\Delta H_I} HOCl \cdot NO_3^- \cdot H_3O^+ \cdot H_2O(aq)$$

$$\Delta H_I = -\Delta H_I^{sr} + \Delta H_I^g + \Delta H_I^{sp}$$

where "sr" and "sp" stand for solvated reactant and solvated product, respectively.

The enthalpies of solvation of reactants and products can be obtained via ab initio polarizable continuum model (PCM)[34] calculations. To estimate the free energy difference between the $HOCl \cdot NO_3^- \cdot H_3O^+ \cdot H_2O$ and $H_2OCl^+ \cdot NO_3^- \cdot (H_2O)_2$ complexes on ice, we fully optimized at the HF/6-31G* level the structure of each species using GAMESS.[35] This step provides the gas-phase reference energies. All the species were then re-optimized

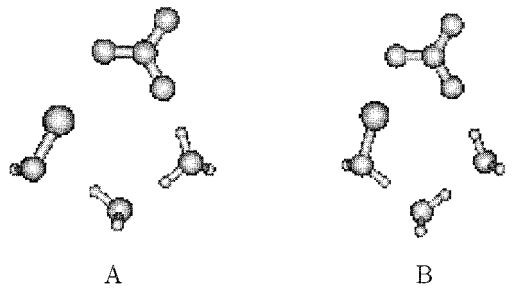

Figure 1. $HOCl{\cdot}NO_3^-{\cdot}H_3O^+{\cdot}H_2O$ (A) and $H_2OCl^+{\cdot}NO_3^-{\cdot}H_2O{\cdot}H_2O$ (B) clusters used in the PCM HF/6-31G* energetic estimates.

within the PCM with cavity radii H 1.44, O 1.8, N 1.92, Cl 2.172 Å and water's dielectric constant $\epsilon = 80$.[36] The two product complexes were then assembled from the PCM-optimized species HOCl, NO_3^-, H_3O^+, H_2OCl^+, and H_2O (cf. Figure 1), and the intermolecular distances were optimized by holding all of the intramolecular coordinates fixed, including the intermolecular angles and torsions, to mimic ice lattice constraints.

We note that these calculations do not yield enthalpy differences. The energy of species in aqueous solution are free energies, whereas the energies of gas phase species are internal energies (or free energies at 0 K). Here we are ignoring these differences; in comparing the two mechanisms, these may, in fact, substantially cancel. Throughout, we also assume that the entropy contributions to the solvation free energies, used in calculating $\Delta H_{I,II}^{sp}$, substantially cancel, because they both refer to cycles with a single ion pair and the same number of moieties. We comment again on this aspect at the conclusion of this section.

The result of these calculations for mechanism I, involving the H_3O^+ ion, is (cf. Table 2) $\Delta H_I^{sp} \simeq \Delta E_I^{sp} = -180.57$ kcal/mol for the product complexation and solvation step. The terms comprising ΔE are the ab initio total (electronic plus nuclear) energy in the gas phase (g) or in a dielectric continuum (aq). For the reactant solvation, we obtain (cf. Table 2) $\Delta H_I^{sr} \simeq \Delta E_I^{sr} = -22.71$ kcal/mol. This gives the reaction enthalpy for mechanism I as $\Delta H_I = 0.84$ kcal/mol. This result is consistent with current estimates from both experiment[9] and theory.[20]

The reaction cycle for mechanism II, involving the H_2OCl^+ ion, is

$$ClONO_2(aq) + 3H_2O(aq) \xrightarrow{-\Delta H_{II}^{sr}} ClONO_2(g) + 3H_2O(g)$$

$$ClONO_2(g) + 3H_2O(g) \xrightarrow{\Delta H_{II}^{g}} H_2OCl^+(g) + NO_3^-(g) + 2H_2O(g)$$

$$H_2OCl^+(g) + NO_3^-(g) + 2H_2O(g) \xrightarrow{\Delta H_{II}^{sp}} H_2OCl^+{\cdot}NO_3^-{\cdot}H_2O{\cdot}H_2O(aq) \quad (2.10)$$

$$ClONO_2(aq) + 3H_2O(aq) \xrightarrow{\Delta H_{II}} H_2OCl^+{\cdot}NO_3^-{\cdot}H_2O{\cdot}H_2O(aq)$$

$$\Delta H_{II} = -\Delta H_{II}^{sr} + \Delta H_{II}^{g} + \Delta H_{II}^{sp}$$

Note that $\Delta H_{II}^{sr} = \Delta H_I^{sr}$, because the reactants are identical for both mechanisms. Here the solvated products contribution ΔH_{II}^{sp} is given by (cf. Table 2) $\Delta H_{II}^{sp} \simeq \Delta E_{II}^{sp} = -177.55$ kcal/mol. The reaction enthalpy for mechanism II is then $\Delta H_{II} = 17.66$ kcal/mol.

This thermodynamic analysis thus shows that the reaction pathway involving H_3O^+ (mechanism I) should be substantially favored over the one involving H_2OCl^+ (mechanism II), because the resulting $HOCl{\cdot}NO_3^-{\cdot}H_3O^+{\cdot}H_2O$ product complex is ~17 kcal/mol more stable than $H_2OCl^+{\cdot}NO_3^-{\cdot}(H_2O)_2$. The basic argument is illustrated in Figure 2, which locates the calculated difference $\Delta H_{II} - \Delta H_I = 16.8$ kcal/mol, associated with the two mechanisms. The hypothetical reaction intermediate $H_2OCl^+{\cdot}NO_3^-$ lies then at $\Delta H_{II} - \Delta H_I - \Delta H_{rxn}$, where ΔH_{rxn} is variously estimated, in kcal/mol, at $\Delta H_{rxn} = -0.6$[20] and -1.6[26] with respect to reactants. This gives a range of 17.4−18.4 kcal/mol for the location of the $H_2OCl^+{\cdot}NO_3^-$ ion pair with respect to reactants. Thus the barrier height $E_{ACT,II}$ for reaching the transition state, TS_{II}, must exceed these values, i.e., $E_{ACT,II} \geq 17.4$ kcal/mol (by taking the lower $\Delta H_{II} - \Delta H_I$ estimate). This is to be contrasted with estimates of the activation energy $E_{ACT,I}$ for mechanism I as 6.6,[30] 3,[20] and 7[26] kcal/mol. Thus the proton-transfer mechanism I is favored over mechanism II involving the H_2OCl^+ ion by 10.4−14.4 kcal/mol, a decisive amount.

Finally, the calculations also show that the intrinsic gas phase bias favoring mechanism I over II is in fact slightly enhanced by solvation and complexation effects. Although our discussion has been largely in terms of enthalpy changes, the entropy changes associated with solvation of the different ion pairs, which is potentially the largest source of entropy change difference in the two mechanisms, are included.

TABLE 2: Energies for $ClONO_2$ Hydrolysis Model Calculations[a]

X	$E[X_{(g)}]$	$E[X_{(aq)}]$[b]
H_2O	−76.010 747	−76.020 938
H_3O^+	−76.286 564	
HOCl	−534.841 967	
H_2OCl^+	−535.097 443	
NO_3^-	−278.912 975	
$ClONO_2$	−738.259 940	−738.265 555
$c[H_3O^+]$[c]	-	−966.340 001
$c[H_2OCl^+]$[c]	-	−966.314 862

[a] All calculations at the HF/6-31G* level. Energies in hartree. See the Supporting Information for details. [b] Obtained from the PCM (ref 34). See text. [c] $c[H_3O^+] = HOCl{\cdot}NO_3^-{\cdot}H_3O^+{\cdot}H_2O$, $c[H_2OCl^+] = H_2OCl^+{\cdot}NO_3^-{\cdot}H_2O{\cdot}H_2O$.

3. Analysis of the Spectroscopic Data

We now turn to the issue of the evidence for the H_2OCl^+ ion's existence on ice from an experimental spectroscopic perspective.

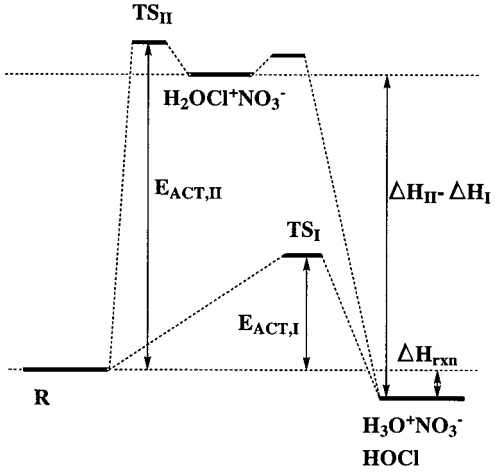

Figure 2. Energetics of the $ClONO_2$ hydrolysis (schematic). R is the reactant complex.

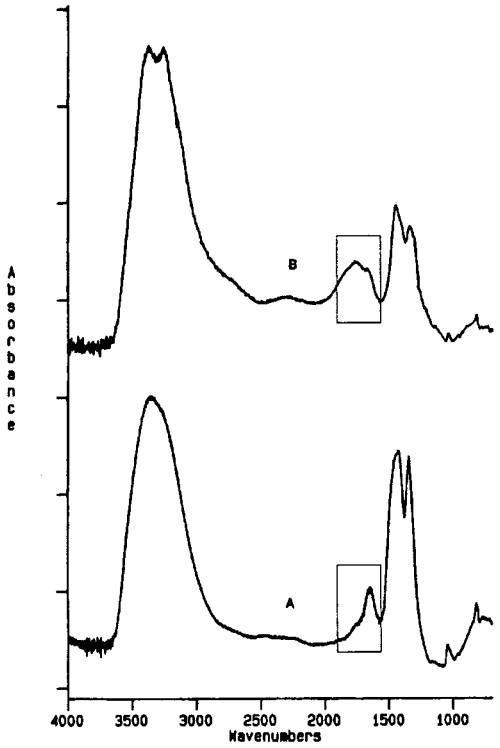

Figure 3. RAIR spectra of condensed reaction product films on a gold foil substrate at 180 K: (A) $ClONO_2$/water ($1.5 \times 10^{-6}/1.5 \times 10^{-7}$ mbar); (B) N_2O_5/water ($4 \times 10^{-7}/3 \times 10^{-6}$ mbar). Reprinted with permission from *J. Phys. Chem.* **1995**, *99*, 6258−6262. Copyright 1995 American Chemical Society. The frames in the 2000−1500 cm^{-1} region, spanning identical frequency ranges, are our addition to guide the eye.

We first very briefly review previous considerations concerning the RAIR spectra and the arguments for and against H_2OCl^+. (We limit discussion of the Sodeau group spectra to those of SHBK at 180 K, originally[11] used to argue for H_2OCl^+, and subsequently cited[13,14] in its support.) First, as noted in the Introduction, the SHBK proposal hinges upon an inference based on a comparison of the spectra of a $ClONO_2/H_2O$ 10:1 mixture and a N_2O_5/H_2O 1:10 mixture at 180 K (Figure 3) in the 1600−1800 cm^{-1} region, which would indicate, according to SHBK, the presence of H_2OCl^+ in the $ClONO_2/H_2O$ mixture.

BH have argued against this and offered some evidence for the presence of molecular HNO_3 in lieu of H_2OCl^+. Specifically, SHBK compared spectra A and B in Figure 3 and contended that the only difference in the frequency patterns was the shift of a 1750 cm^{-1} broad peak in the N_2O_5 spectrum, agreed by all to be a H_3O^+ feature, to a 1650 cm^{-1} sharp peak in the $ClONO_2$ spectrum, assigned *by analogy* (with H_3O^+) to H_2OCl^+, thus implying that the ice surface contained Cl species. BH noted instead that *both* the 1750 and the 1650 peaks are in fact present in *both* spectra. BH argued that, since the A and B absorption patterns contain features at the same frequencies (with intensities modulated by the degree of solvation of the N_2O_5 and $ClONO_2$ hydrolysis products), the RAIR sample corresponding to spectrum A cannot contain any Cl species.[37] Thus, in contrast to SHBK, BH interpreted both spectra as typical of $HNO_3/H_3O^+/NO_3^-/H_2O$ mixtures with different degrees of acid ionization, none containing chlorine species, because BH assumed that HOCl had desorbed from the ice, and assigned the 1650 peak to molecular HNO_3, although the specific HNO_3 vibrational mode was not identified by BH.

In this section, we address in some detail the spectroscopic identification of H_2OCl^+ and HNO_3. Our procedure is the following: (i) present typical IR features of HNO_3, H_3O^+, and NO_3^- on ice, (ii) identify these features in Figure 3B, where all agree that no chlorine is present, and finally, in light of these identifications, (iii) assign the features in Figure 3A. Our examination of relevant IR spectra shows that the features previously attributed to H_2OCl^+ can be convincingly assigned to HNO_3.

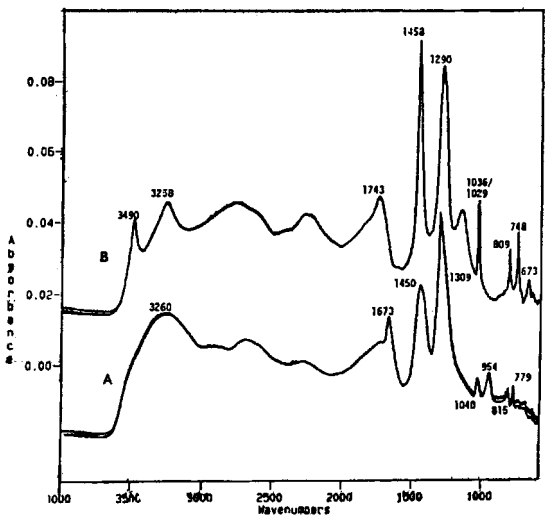

Figure 4. Infrared spectra of clusters having a 2:1 water/HNO_3 ratio: (A) superimposed spectra of amorphous clusters formed at 165 K and aged 2, 7, and 14 min; (B) superimposed spectra of crystalline NAD clusters formed at 175 K and aged 2, 7, and 10 min. Spectra have been offset by ±0.02 for clarity. Reprinted with permission from *J. Phys. Chem.* **1993**, *97*, 5848−5851. Copyright 1993 American Chemical Society.

3.1. IR Features of HNO_3, H_3O^+, and NO_3^- on Ice. Here we first examine the IR spectra of molecular nitric acid and its ionization products on ice to establish the characteristic spectral features of all of these species in an ice environment. To begin, it is useful to refer to the HNO_3 and $H_3O^+NO_3^-$ spectroscopic features for 2:1 H_2O/HNO_3 samples, shown in Figure 4. (Here and henceforth, the designation "HNO_3" represents undissociated, molecular HNO_3.) These reference spectra are relevant because the samples in the experiments carried out by SHBK are likely to yield spectra similar to amorphous NAD, Figure 4A, or amorphous NAT,[39] because of their preparation via chemical reaction at the surface.

In Figure 4, trace A refers to a sample containing mostly HNO_3, with the characteristic absorption pattern[38]

$$HNO_3\text{: } 1673, 1450, 1309, 954, 779 \text{ (Figure 4A)} \quad (3.11)$$

Trace B of Figure 4 shows the absorption pattern of a sample containing mostly $H_3O^+NO_3^-$:

$$H_3O^+\text{: } 1743 \text{ (Figure 4B)} \quad (3.12)$$

$$NO_3^-\text{: } 1458, 1290, 1036/1029, 809 \text{ (Figure 4B)} \quad (3.13)$$

With the knowledge of these typical absorption patterns, we now examine the spectra in Figure 3, where the sole proposed representative spectral feature of H_2OCl^+, a narrow band at 1650 cm^{-1}, was first assigned.[11] We deal first with spectrum B (N_2O_5/H_2O 1:10) to discuss the HNO_3 and NO_3^- bands and then discuss spectrum A ($ClONO_2/H_2O$ 10:1).

3.2. Examination of Figure 3, Trace B. In Figure 3B, the absorption patterns of HNO_3 and $H_3O^+NO_3^-$ appear together.

HNO_3 bands are seen at

$$HNO_3\text{: } 1650, 1420, 1330, 960, 770 \text{ (Figure 3B)} \quad (3.14)$$

$$HNO_3\text{: } 1673, 1450, 1309, 954, 779 \text{ (Figure 4A)} \quad (3.15)$$

whereas H_3O^+ and NO_3^- bands are seen at

$$H_3O^+\text{: } 1750 \text{ (Figure 3B)} \quad (3.16)$$

$$H_3O^+\text{: } 1743 \text{ (Figure 4B)} \quad (3.17)$$

$$NO_3^-\text{: } 1450, 1290, 1040, 820 \text{ (Figure 3B)} \quad (3.18)$$

$$NO_3^-\text{: } 1458, 1290, 1036/1029, 809 \text{ (Figure 4B)} \quad (3.19)$$

where for the reader's convenience we have also reported the reference absorption patterns of Figure 4 underneath the corresponding ones from Figure 3. Note that all the bands are slightly shifted from respectively Figure 4A (mostly HNO_3) and Figure 4B (mostly $H_3O^+NO_3^-$) because of differences in experimental conditions.

It should be remarked that the intensities of the HNO_3 bands at 960 and the NO_3^- bands at 1040 and 820 in Figure 3B, although primarily due to the concentration of the corresponding species, are also significantly influenced by the water background (see e.g., Figure 1 in ref 40). The water background presents two peaks relevant to our discussion: (i) at 900 cm^{-1}, spanning the 700−1000 cm^{-1} range and (ii) at 1645 cm^{-1}, spanning the broader 1000−2000 cm^{-1} range, and about half as intense as the 900 cm^{-1} peak. The 960(HNO_3), 820(NO_3^-), and 770(HNO_3) bands in Figure 3B are enhanced and distorted by the 900 water peak, whereas the 1650 peak is ehanced by the 1645 water background broad band more than the 1750 peak. (The issue of the water background will appear again in the discussion below.)

3.3. Examination of Figure 3, Trace A. We now turn to Figure 3A and analyze three adjacent regions of the spectrum separately.

1800−1600 cm^{-1} Region. Evidence for the presence of H_3O^+ is the 1750 band (cf. eqs 3.16 and 3.17), which appears as a shoulder of the 1650 band. (Why the hydronium ion 1750 band is not more pronounced is related to the water background effect mentioned in section 3.2, and will be further commented upon below.) The 1650 feature is interpreted as HNO_3 in the BH scenario (cf. eqs 3.14 and 3.15) and not as H_2OCl^+ (as in the SHBK view). Consistency requirements for the identifications just made in Figure 3A are (a) that the counterion NO_3^- should be reflected in the spectrum to a degree consistent with H_3O^+ and (b) that any ionized nitric acid must come at the expense of molecular HNO_3; both issues are addressed in the following two spectral region discussions.

1600−1100 cm^{-1} Region. The general features of importance in this region are that, as one goes from Figure 3B to Figure 3A, the NO_3^- band intensities decrease, whereas the HNO_3 band intensities increase, consistent with the H_3O^+ behavior in the 1700−1600 region just discussed. The details of this are as follows. Relying on our assignment for NO_3^- and HNO_3 in section 3.2, on going from B to A, the intensities of 1450(NO_3^-) and 1290(NO_3^-) have decreased with respect to 1420(HNO_3) and 1330(HNO_3) because of the lower water content. The 1330 band is characteristic (cf. eqs 3.14 and 3.15) of HNO_3,[40−42] whereas NO_3^- has a band at lower frequency, clearly visible in B at 1290 as a shoulder on the 1330 band.

TABLE 3: B3LYP/6-311++G(d,p) Bond Lengths in the $H_2O{\cdot}ClONO_2$ Subsystem in Water Clusters from Ref 26

	gas	A[a]	B	C	D	E
R_{ClO}[b]	1.71[c]	1.79	1.91	1.91	1.90	2.09
R_{OCl}	1.77[d]	2.34	2.11	2.07	2.13	1.93

[a] The parameters for cases A−E correspond to Figures 3−6 and 8, respectively, in ref 26. Bond lengths in Å. [b] R_{ClO} = Cl−ONO_2 bond; R_{OCl} = H_2O−Cl bond. [c] $ClONO_2$ from Table 3 in ref 26. [d] H_2OCl^+ from Table 2 in ref 26.

1100−700 cm^{-1} Region. The important general features in this region are again those of the NO_3^-/HNO_3 behavior and are the same as in the 1600−1100 region just discussed. We begin the discussion by focusing on the bands identified in Figure 3B (cf. eqs 3.14−3.19): 1040(NO_3^-), 960(HNO_3), 820(NO_3^-), and 770(HNO_3). The decrease in intensity, expected in the BH scenario, of 1040(NO_3^-) and 820(NO_3^-) relative to 960(HNO_3) and 770(HNO_3) going from Figure 3B to Figure 3A can only be appreciated with difficulty, because of both the distortion by the ice spectrum as discussed above and the related spectral calibration issue as now addressed.

We conclude with some remarks relevant for the three spectral regions. Care is required in comparing the intensities in the two spectra A and B in Figure 3, because the absorption maximum in each spectrum is attuned to the predominant water peak at 3300, which renders the NO_3^-/HNO_3 absorptions in Figure 3B artificially less intense than those in Figure 3A: the 1040(NO_3^-) band in Figure 3B should in fact be more intense than the same band in Figure 3A because of the larger water content of the former mixture. This observation is a key point in recognizing the decrease in intensity of 1750(H_3O^+) coincident with the decrease of the 1040(NO_3^-) and 820(NO_3^-) bands. At first sight, 1040(NO_3^-) seems more intense in Figure 3A than in Figure 3B: this is because the two spectra are not calibrated with respect to the nitrate group bands. In fact, 1040(NO_3^-) should appear more intense in Figure 3B, because of a higher concentration of NO_3^-.

In view of the discussion above, it is clear in our view that H_3O^+ is indeed present in Figure 3A and is the counterion for NO_3^- and that the H_3O^+, NO_3^-, and HNO_3 absorption patterns on going from Figure 3B to Figure 3A are all internally consistent with this. It follows that in Figure 3A 1650 is molecular HNO_3 and not H_2OCl^+.[43]

4. Further Theoretical Considerations and Assignment of the Vibrational Bands of HNO_3, NO_3^-, and H_3O^+ on Ice

In this section, we present theoretical calculations to support the identifications made in section 3 and to identify the key vibrational modes involved, in particular the 1650 mode. Before proceeding, it is important to make several relevant considerations. Beyond the fact that RAIR spectra for the same systems vary somewhat (tens of cm^{-1}) with experimental conditions,[11,27,44] even high level ab initio calculations of IR frequencies for small polyatomics are only accurate to within tens of cm^{-1}.[45] Accordingly, the calculations for complex solute-cluster systems focus on approximate frequencies but with special attention given to the overall patterns of the spectra and the band assignments of the individual modes.

TABLE 4: HNO_3 Vibrational Frequencies in Water Clusters[a]

mode		HNO_3[b]	$HNO_3\cdot(H_2O)_n$ $n=3$	$HNO_3\cdot(H_2O)_n$ $n=6$	Figure 3B eq 3.14	Figure 4A eq 3.15	I[c]
OH str	ν_1	3550 (0.8819)	3028	2776			42.37
NO_2 a-str	ν_2	1710 (0.8640)	1702	1699	1650	1673	10.11
NO_2 s-str	ν_3	1326 (0.8246)	1352	1367	1330	1309	12.65
HON ben	ν_4	1304 (0.8662)	1390	1390	1420	1450	7.69
NO_2 ben in	ν_5[d]	647 (0.7724)	911	918	960	954	1.23
$O-NO_2$ str	ν_6	879 (0.8262)	654	656			0.13
$O-NO_2$ ben	ν_7	580 (0.8469)	623	629			2.02
NO_2 ben out	ν_8[d]	763 (0.8396)	775	778	770	779	1.02
OH tor	ν_9	458 (0.8327)	809	923			5.75

[a] All frequencies in cm^{-1}. HF/6-31G* frequencies unless otherwise specified. [b] HNO_3 experimental frequencies and assignments from McGraw, G. E; Bernitt, P. L.; Hisatsune, I. C. *J. Chem. Phys.* **1965**, *42*, 237. HF/6-31G* frequencies scaling factors in parentheses. The unscaled HF/6-31G* frequencies can be obtained by dividing the reported frequencies by their associated scaling factors. The latter are quite similar to the 0.8953 scaling factor recommended for HF/6-31G* vibrational frequencies.[45] [c] HF/6-31G* intensities in D^2 amu^{-1} $Å^{-2}$. [d] "in": in plane; "out": out of plane. See the Supporting Information for details.

Our starting point is a very recent theoretical study on the $ClONO_2$ hydrolysis by McNamara and Hillier[26] (MH). We first stress that the reaction path aspects of the MH study confirm the BH proton-transfer picture of the mechanism via nucleophilic attack by an OH^--like species rather than H_2O, as can be verified by a comparison of Figure 10 of ref 26 and Figures 2 and 3 of ref 20 for the reaction transition state. However, MH also present assorted non-reaction-path studies of various water clusters containing $ClONO_2$. Some of these, Figures 3−6 of ref 26, are stated to "support" the existence of the H_2OCl^+ ion. However, from the examination of Table 3, based on these figures, it is clear that in cases A−D the water oxygen is always *farther* away from Cl than is the nitrate oxygen, and thus inconsistent with an H_2OCl^+ ion. Case E is explicitly identified by MH as involving the H_2OCl^+ ion. However, the structure of the complex in case E is biased toward a high degree of solvation of all of the oxygens of $ClONO_2$, engaging the nitrate group electron density and making it less available for $Cl^{\delta+}$, and has an ad hoc coordination of the attacking water to the solvating waters, which maximizes its nucleophilicity. In any event, this complex cannot be accessed via the transition state displayed in Figure 10 of ref 26 because the proton of the attacking water is transferred *during* the nucleophilic attack along a lower energy pathway.

MH also report an (incomplete) set of calculated vibrational frequencies for the H_2OCl^+ moiety identified in the $ClONO_2\cdot(H_2O)_8$ cluster of case E in Table 3 (cf. Table 8 in ref 26). The reported 484/1408/2322/2914 cm^{-1} absorption pattern fails to match that of Figure 3A and especially the band at 1650 cm^{-1}, which in the SHBK view reflects H_2OCl^+, but in the BH view does not.

Since, as detailed in Section 3, our thesis is that the 1650 band is HNO_3 (the HNO_3 absorption pattern was not reported in ref 26), we have calculated using GAMESS[35] the vibrational frequencies of HNO_3 both isolated and in $HNO_3\cdot(H_2O)_{3,6}$ clusters for comparison with the spectra in Figures 3B and 4B, and in particular with the 1650 feature, to further examine our assignments made in section 3. In Table 4, we report the frequencies for the HNO_3 moiety in the three cases. We have scaled independently each calculated frequency for gas-phase HNO_3 to match exactly the corresponding experimental frequency. We then have identified by inspection, using MacMolplot[46] and Molden,[47] the HNO_3 moiety's modes in the water clusters and scaled the corresponding frequencies by the factors obtained for gas-phase HNO_3 (cf. Table 4, col 2).

Table 4 shows that the calculated absorption patterns reproduce quite well the experimental patterns of Figures 3B and 4A, supporting the HNO_3 band identifications that we made in section 3, including the key band in the 1650 cm^{-1} neighborhood.[50]

TABLE 5: NO_3^- and H_3O^+ Vibrational Frequencies in the $H_3O^+\cdot NO_3^-\cdot(H_2O)_7$ Clusters[a]

mode		Figure 3B eq 3.18	Figure 4B eq 3.13	NO_3^-[c]	I[b]
NO_2 a-str	ν_2[d]	1450	1458	1457	15.43
NO_2 s-str	ν_3	1040	1029	1030	0.44
NO_2 ben in	ν_5			647	1.95
$O-NO_2$ str	ν_6	1290	1290	1337	12.28
$O-NO_2$ ben	ν_7			693	0.97
NO_2 ben out	ν_8	820	809	821	0.68
		eq 3.16	eq 3.17	H_3O^+[e]	
H_3O^+ s-str	ν_1			2461	56.49
H_3O^+ s-ben	ν_2			1318	12.16
OH_2 a-str	ν_3			2980	43.16
OH_2 a-str	ν_3'			3087	20.72
HOH a-ben	ν_4	1750	1743	1700	0.33
HOH s-ben	ν_4'			1697	1.03

[a] All frequencies at the HF/6-31G* level unless otherwise specified. [b] HF/6-31G* intensities in D^2/(amu $Å^2$). [c] HNO_3-scaled. See scaling factors for each mode reported in Table 4. [d] Nomenclature of the nitrate group bands as in Table 4. [e] The scaling factors for the H_3O^+ frequencies (0.8732 bend, 0.8975 stretch) have been obtained by comparing H_2O HF/6-31G* frequencies (1826.55, 4070.46, and 4188.71) to the experimental water frequencies (1595, 3657, and 3756).[48]

To show that NO_3^- does not have features in the vicinity of 1650 that would compromise the key HNO_3 band identification, we have calculated the IR spectrum of the $H_3O^+\cdot NO_3^-\cdot(H_2O)_7$ complex at the HF/6-31G* level to compare with the IR patterns eqs 3.13 and 3.18. The calculated absorption pattern reported in Table 5 indicates that there is indeed no NO_3^- activity in the 1650 region and consistently reproduces the experimental one, confirming our assignment of the 1650 band in Figure 3A.[51] Furthermore, Table 5 supports all of the NO_3^- and H_3O^+ assignments discussed in section 3. Figures 5−7 depict the nuclear motions corresponding to the calculated frequencies of HNO_3, NO_3^-, and H_3O^+. Figure 8 collects the HNO_3, NO_3^-, and H_3O^+ calculated IR absorption patterns from Tables 4 and 5.

These calculations provide a further important new piece of information: the 1650 band in Figure 3A corresponds with the NO_2 asymmetric stretch ν_2 of molecular HNO_3 (cf. Table 4, column 4, 1699 peak). Although the H_3O^+ ion also has a calculated absorption at 1700 cm^{-1} (cf. Table 5, column 4), its calculated intensity of 0.33 D^2 amu^{-1} $Å^{-2}$ is too low compared to the experimental one in ref 39, which is instead best matched by the NO_2 ν_2 vibration's corresponding intensity of 10.11 D^2 amu^{-1} $Å^{-2}$ in Table 4.

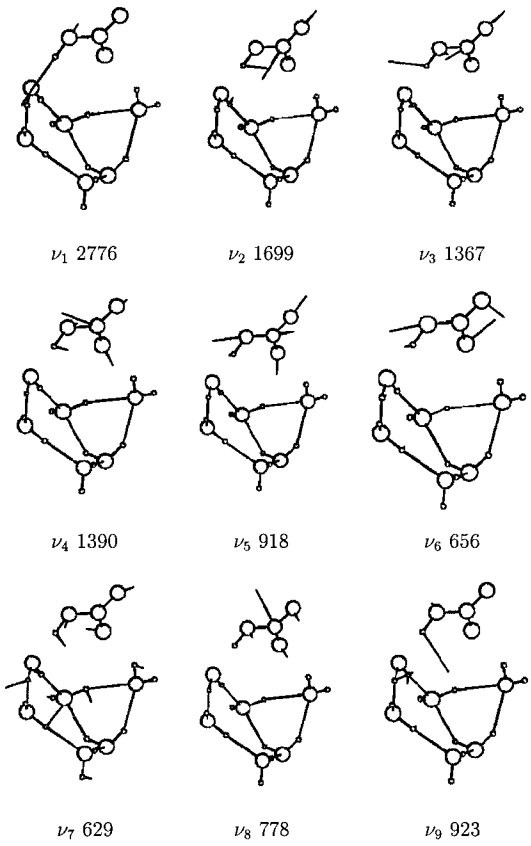

Figure 5. HNO_3 normal modes in the $HNO_3 \cdot (H_2O)_6$ complex (from Table 4).

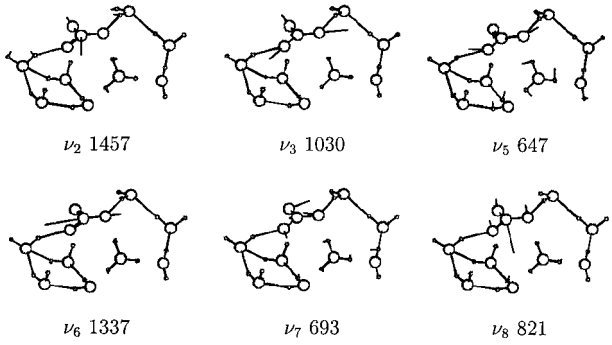

Figure 6. NO_3^- normal modes in the $H_3O^+ \cdot NO_3^- \cdot (H_2O)_7$ complex (from Table 5).

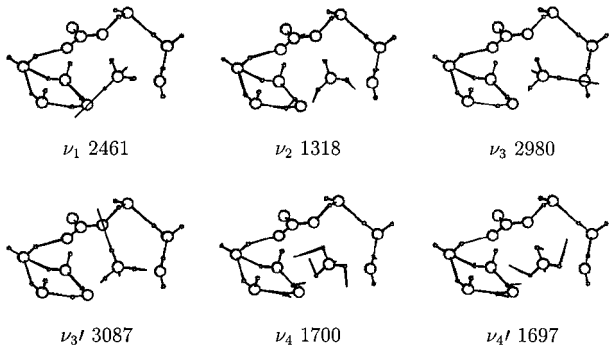

Figure 7. H_3O^+ normal modes in the $H_3O^+ \cdot NO_3^- \cdot (H_2O)_7$ complex (from Table 5).

5. Concluding Remarks

In this paper, we have presented new thermodynamic, calculational, and IR considerations that indicate that the H_2OCl^+ ion is not involved in the $ClONO_2$ hydrolysis on ice surfaces. We have also presented IR spectra calculations providing an explicit identification of the 1650 cm^{-1} spectral feature. Overall, the present results lend independent support to the proton-transfer mechanism for $ClONO_2$ hydrolysis originally found in ref 20.[52]

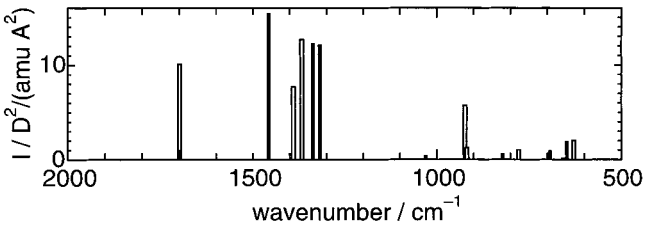

Figure 8. HNO_3, NO_3^-, and H_3O^+ calculated IR absorption patterns. Empty bars: HNO_3 (from Table 4). Solid bars: NO_3^- and H_3O^+ (from Table 5).

We can suggest two experimental avenues to shed further light on the present issues. First, insight on the presence or absence of H_2OCl^+ could be gained by probing, at $T \approx 180$ K, the region below 700 cm^{-1}, where any Cl−O stretch should be visible. Although there can also be, for example, HNO_3 activity in this region (cf. Tables 4 and 5 and Figure 8), at least a further spectral window could be explored to check the overall consistency of IR assignments. RAIR spectra in this region were not reported for $ClONO_2/H_2O$ samples in ref 11, but the capability appears to exist at least down to 500 cm^{-1}.[13]

Second, we have identified the key 1650 cm^{-1} feature assigned to molecular HNO_3 by BH as an NO_2 asymmetric stretch of molecular HNO_3, whereas it as assigned as a H_2OCl^+ bend in the SHBK scenario. The asymmetric stretch of NO_2 in the neutral HNO_3 (solvated) molecule should not change much if every H in the system is replaced by D (there will be a small effect because H_2O and D_2O do not solvate to the same degree); no significant H/D isotope effect would be seen. On the other hand, for the bending or wag vibrations in H_2OCl^+,[33] there are significant motions of the two H's, and accordingly, an expected H/D isotope effect lowering the vibrational frequency by a factor close to $1/\sqrt{2}$, Thus, a RAIR experiment on D_2O ice would shed further light on the identity of the 1650 cm^{-1} band.

Acknowledgment. This work was supported in part by NSF grants ATM-9613802, ATM-0000542,CHE-9700419, and CHE-9709195.

Supporting Information Available: Structures, energies, and frequencies of the gas-phase species HNO_3, $HNO_3 \cdot (H_2O)_{2,3,6}$, and $H_3O^+ \cdot NO_3^- \cdot (H_2O)_7$. Structures of the aqueous species $HOCl \cdot NO_3^- \cdot H_3O^+ \cdot H_2O$ and $H_2OCl^+ \cdot NO_3^- \cdot (H_2O)_2$. This material is available free of charge via the Internet at http://pubs.acs.org.

References and Notes

(1) Molina, M. J.; Tso, T. L.; Molina, L. T.; Wang, F. C. Y. *Science* **1987**, *238*, 1253.

(2) Chu, L. T.; Leu, M.-T.; Keyser, L. F. *J. Phys. Chem.* **1993**, *97*, 12798. Leu, M.-T.; Moore, S. B.; Keyser, L. F. *J. Phys. Chem.* **1991**, *95*, 7763.

(3) Tolbert, M. A.; Rossi, M. J.; Malhotra, R.; Golden, D. M. *Science* **1987**, *238*, 1258.

(4) Leu, M.-T. *Geophys. Res. Lett.* **1988**, *15*, 17.

(5) Hanson, D. R.; Ravishankara, A. R. *J. Geophys. Res.* **1991**, *96*, 5081.

(6) Barone, S. B.; Zondlo, M. A.; Tolbert, M. A. *J. Phys. Chem. A* **1997**, *101*, 8643.

(7) Hanson, D. R. *J. Phys. Chem.* **1995**, *99*, 13059.

(8) Oppliger, R.; Allanic, A.; Rossi, M. J. *J. Phys. Chem. A* **1997**, *101*, 1903.
(9) Hanson, D. R.; Ravishankara, A. R. *J. Phys. Chem.* **1992**, *96*, 2682.
(10) Abbatt, J. P. D.; Molina, M. J. *J. Phys. Chem.* **1992**, *96*, 7674.
(11) Sodeau, J. R.; Horn, A. B.; Banham, S. F.; Koch, T. G. *J. Phys. Chem.* **1995**, *99*, 6258.
(12) Banham, S. F.; Horn, A. B.; Koch, T. G.; Sodeau, J. R. *Faraday Discuss.* **1995**, *100*, 321.
(13) Horn, A. B.; Sodeau, J. R.; Roddis, T. B.; Williams, N. A. *J. Phys. Chem. A* **1998**, *102*, 6107.
(14) Horn, A. B.; Sodeau, J. R.; Roddis, T. B.; Williams, N. A. *J. Chem. Soc., Faraday Trans.* **1998**, *94*, 1721.
(15) For recent reviews, see: Molina, M. J.; Molina, L. T.; Kolb, C. E. *Annu. Rev. Phys. Chem*. **1996**, *47*, 327. Peter, Th. *Annu. Rev. Phys. Chem*. **1997**, *48*, 785. Solomon, S. *Rev. Geophys.* **1999**, *37*, 275.
(16) Schindler, Th.; Berg, Ch.; Niedner-Schatteburg, G.; Bondybey, V. E. *J. Chem. Phys.* **1996**, *104*, 3998.
(17) Geiger, F. M.; Tridico, A. C.; Hicks, J. M. *J. Phys. Chem. B* **1999**, *103*, 8205.
(18) Robinson, G. N.; Worsnop, D. R.; Jayne, J. T.; Kolb, C. E.; Davidovits, P. *J. Geophys. Res.* **1997**, *102*, 3583.
(19) La Manna, G. *THEOCHEM* **1994**, *309*, 31.
(20) Bianco, R.; Hynes, J. T. *J. Phys. Chem. A* **1998**, *102*, 309.
(21) Bianco, R.; Gertner, B. J.; Hynes, J. T. *Ber. Bunsen-Ges. Phys. Chem.* **1998**, *102*, 518.
(22) Bianco, R.; Hynes, J. T. *Int. J. Quantum Chem.* **1999**, *75*, 683.
(23) Akhmatskaya, E. V.; Apps, C. J.; Hillier, I. H.; Masters, A. J.; Palmer, I. J.; Watt, N. E.; Vincent, M. A.; Whitehead, J. C. *J. Chem. Soc., Faraday Trans.* **1997**, *93*, 2775.
(24) Ying, L. M.; Zhao, X. S. *J. Phys. Chem. A* **1997**, *101*, 6807. Xu, S. C.; Zhao, X. S. *J. Phys. Chem. A* **1999**, *103*, 2100.
(25) McNamara, J. P.; Tresadern, G.; Hillier, I. H. *Chem. Phys. Lett.* **1999**, *310*, 265.
(26) McNamara, J. P.; Hillier, I. H. *J. Phys. Chem. A* **1999**, *103*, 7310.
(27) Koch, T. G.; Banham, S. F.; Sodeau, J. R.; Horn, A. B.; McCoustra, M. R. S.; Chesters, M. A. *J. Geophys. Res.* **1997**, *102*, 1513.
(28) March, J. *Advanced Organic Chemistry*, 4th ed.; Wiley: New York, 1992; p 653.
(29) Eigen, M.; Kustin, K. *J. Am. Chem. Soc.* **1962**, *84*, 1355.
(30) Tabazadeh, A.; Turco, R. P. *J. Geophys. Res.* **1993**, *98*, 12727. See also: Henson, B. F.; Wilson, K. R.; Robinson, J. M. *Geophys. Res. Lett.* **1996**, *23*, 1021 and references therein.
(31) Berland, B. S.; Tolbert, M. A.; George, S. M. *J. Phys. Chem. A* **1997**, *101*, 9954.
(32) Lias, S. G.; Bartmess, J. E.; Liebman, J. F.; Holmes, J. L.; Levin, R. D.; Mallard, W. G. *J. Phys. Chem. Ref. Data* **1988**, *17*, 1.
(33) Francisco, J. S.; Sander, S. P. *J. Chem. Phys.* **1995**, *102*, 9615.
(34) Miertus, S.; Scrocco, E.; Tomasi, J. *Chem. Phys.* **1981**, *55*, 117. Tomasi, J.; Persico, M. *Chem. Rev.* **1994**, *94*, 2027. Cammi, R.; Tomasi, J. *J. Comput. Chem.* **1995**, *16*, 1449.
(35) Schmidt, M. W.; Baldridge, K. K.; Boatz, J. A.; Elbert, S. T.; Gordon, M. S.; Jensen, J. H.; Koseki, S.; Matsunaga, N.; Nguyen, K. A.; Su, S. J.; Windus, T. L.; Dupuis, M.; Montgomery, J. A. *J. Comput. Chem.* **1993**, *14*, 1347.
(36) There would be a negligible difference in the current estimates if the ice dielectric constant at 180−190 K were used instead, because the dielectric continuum solvation effect saturates for $\epsilon \approx 20$.
(37) The mass-spectroscopic detection of Cl-containing species observed in ref 11 when water is added to the $ClONO_2/H_2O$ 10:1 mixture does not prove that chlorine compounds have reactively evolved *exclusively* from the IR-monitored ice-covered gold plate surface since, as argued in ref 20, they could have been produced in the hydrolysis of unreacted $ClONO_2$ adsorbed *elsewhere* in the cell.
(38) Absorption frequencies in cm^{-1}. To avoid burdening the text, we simply identify a peak by its wavenumber, often omitting the words *band* and *peak*.
(39) Ritzhaupt, G.; Devlin, J. P. *J. Phys. Chem.* **1991**, *95*, 90.
(40) Horn, A. B.; Koch, T. G.; Chesters, M. A.; McCoustra, M. R. S.; Sodeau, J. R. *J. Phys. Chem.* **1994**, *98*, 946.
(41) Barton, N.; Rowland, B.; Devlin, J. P. *J. Phys. Chem.* **1993**, *97*, 5848.
(42) Koehler, B. G.; Middlebrook, A. M.; Tolbert, M. A. *J. Geophys. Res*. **1992**, *97*, 8065.
(43) Further support to our assignment of spectrum A comes from the RAIR spectrum of a 3/1 mixture of H_2O/N_2O_5 at 170 K reported in ref 27 (Figure 4, trace E), which displays the absorption pattern 1750/1670/1430/1310, strikingly similar to that in the same region of Figure 3A, likely because of a water content lower than in Figure 3B.
(44) Greenler, R. G. *J. Chem. Phys.* **1966**, *44*, 310.
(45) Scott, A. P.; Radom, L. *J. Phys. Chem.* **1996**, *100*, 16502.
(46) Bode, B. M.; Gordon, M. S. *J. Mol. Graphics Mod*. **1999**, *16*, 133.
(47) Schaftenaar, G. Quantum Chemistry Program Exchange. Program no. 619. *MOLDEN: A Portable Electron Density Program*. See also on the Web: http://www.caos.kun.nl/∼schaft/molden/molden.html.
(48) Shimanouchi, T. *Tables of Molecular Vibrational Frequencies Consolidated*; National Bureau of Standards, U.S. Government Printing Office: Washington DC, 1972; Vol. I, pp 1−160.
(49) Ebner, C.; Sansone, R.; Probst, M. *Int. J. Quantum Chem.* **1996**, *70*, 877.
(50) The lack of inclusion of electron correlation and diffused functions, both important for hydrogen-bonded systems, does not affect our results and conclusions with respect to the absorption patterns. We have verified this by comparing the frequencies of the HNO_3 moiety in the $HNO_3 \cdot (H_2O)_2$ complex obtained via the same procedure applied for Table 5 at both HF/6-31G* and MP2/6-31+G* levels. The agreement of the mode-scaled frequencies in the two sets is quite good, in particular in the region above 1500 cm^{-1} (see the Supporting Information for details).
(51) The experimental absorption pattern of the NO_3^- moiety is also well reproduced if the HF/6-31G* NO_3^- frequencies in the $H_3O^+ \cdot NO_3^- \cdot (H_2O)_7$ complex are scaled by factors obtained by comparing $NO_3^- \cdot H_2O$ HF/6-31G* frequencies to the experimental NO_3^- IR signature in solution, cf. Figure 1b and Table 1 in ref 49.
(52) A similar proton-transfer mechanism has been predicted in one variant of the $HCl + ClONO_2$ reaction on ice [Bianco, R.; Hynes, J. T. *J. Phys. Chem. A* **1999**, *103*, 3797] and implicated in the hydrolysis of N_2O_5 on ice (ref 22).